Electronic Supplementary Information

Isoreticular Tp*-W-Cu-S cluster-based one-dimensional coordination polymers with an uncommon [Tp*WS_3Cu_2] + [Cu] combination and their third-order nonlinear optical properties

Quan Liu,[a] Hong-Juan Xu,[a] Li-Ce Yu,[a] Ming-Jie Lu,[a] Yan-Fang Shang,[a] Ying-Lin Song,[c] Wen-Hua Zhang,*[b] and Jian-Ping Lang*[b]

[a] *College of Chemistry and Chemical Engineering, Nantong University, Nantong 226019, China*

[b] *State and Local Joint Engineering Laboratory for Novel Functional Polymeric Materials, College of Chemistry, Chemical Engineering and Materials Science, Soochow University, Suzhou 215123, China*

[c] *School of Physical Science and Technology, Soochow University, Suzhou 215006, China*

Table of Contents

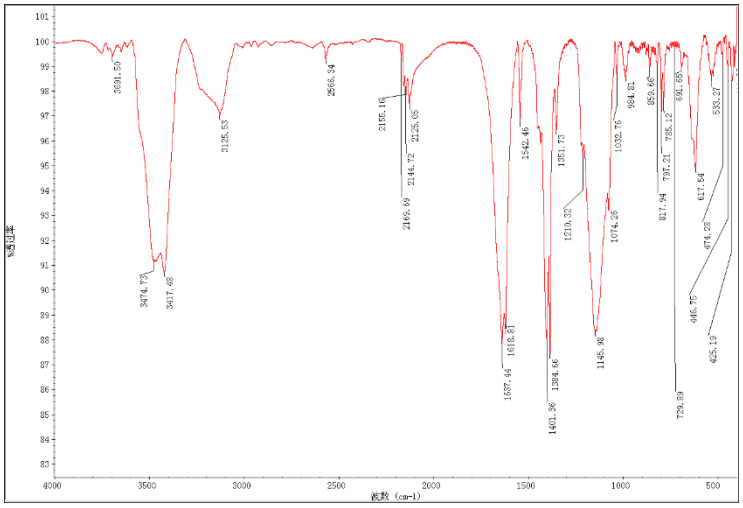

Fig. S1 The FT-IR spectrum of **2**.

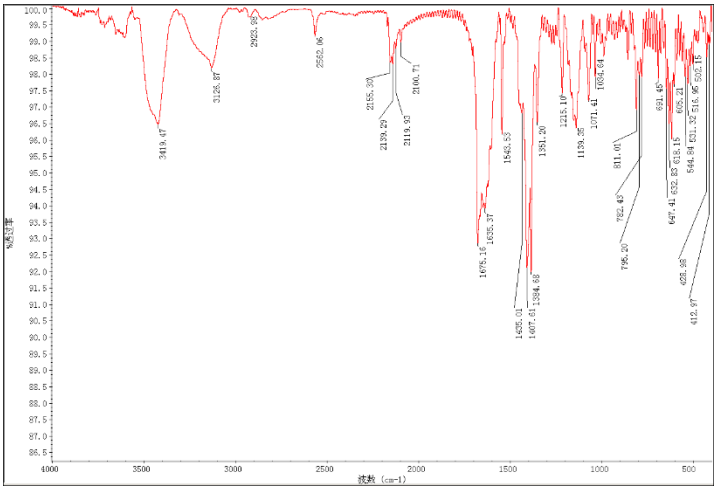

Fig. S2 The FT-IR spectrum of **3**.

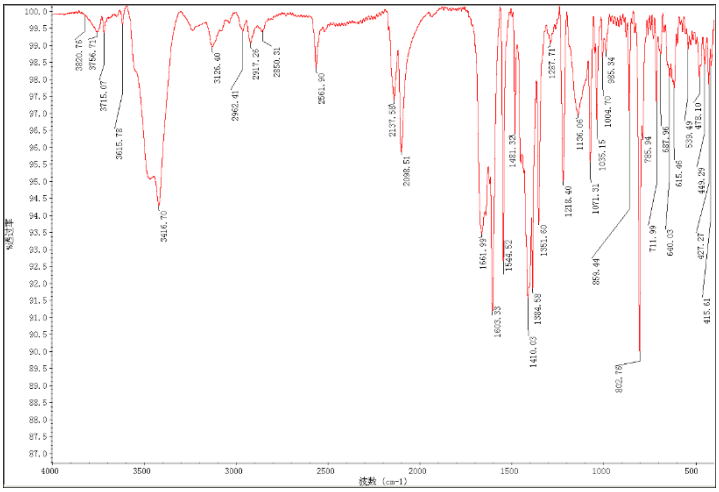

Fig. S3 The FT-IR spectrum of **4**.

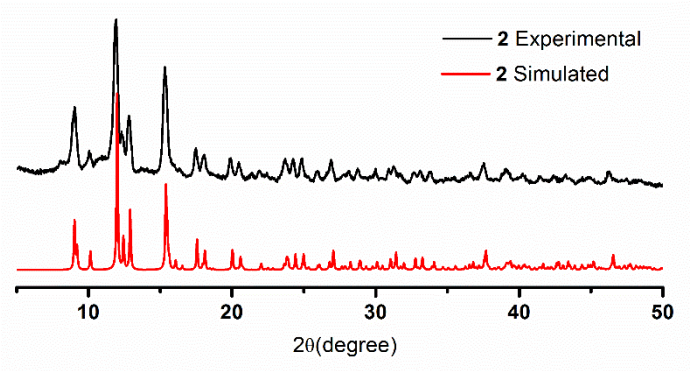

Fig. S4 The PXRD pattern of **2**, showing a good consistency between the experimental and the simulated diffraction patterns.

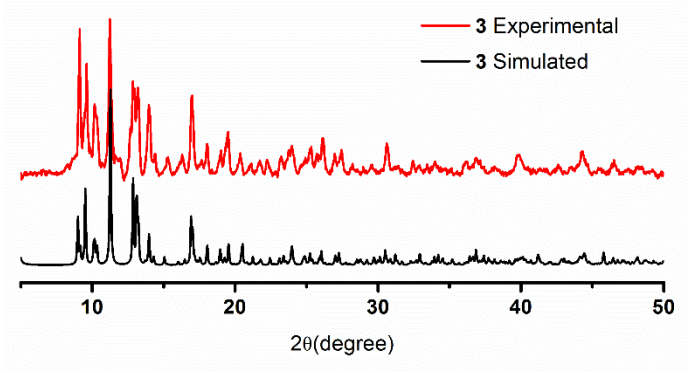

Fig. S5 The PXRD pattern of **3**, showing a good consistency between the experimental and the simulated diffraction patterns.

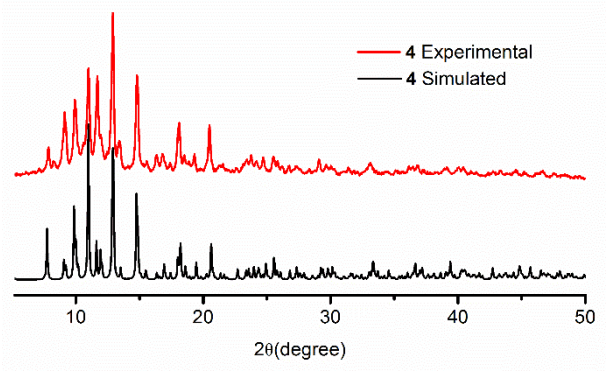

Fig. S6 The PXRD pattern of **4**, showing a good consistency between the experimental and the simulated diffraction patterns.

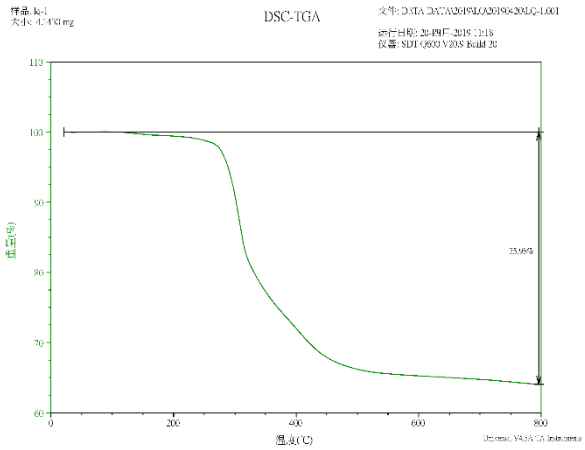

Fig. S7 The TGA curve of **2**.

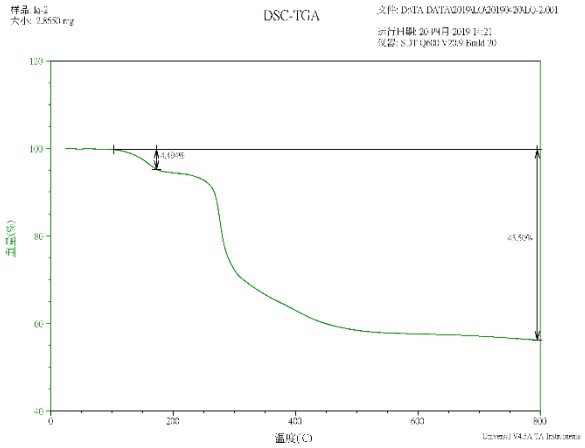

Fig. S8 The TGA curve of **3**.

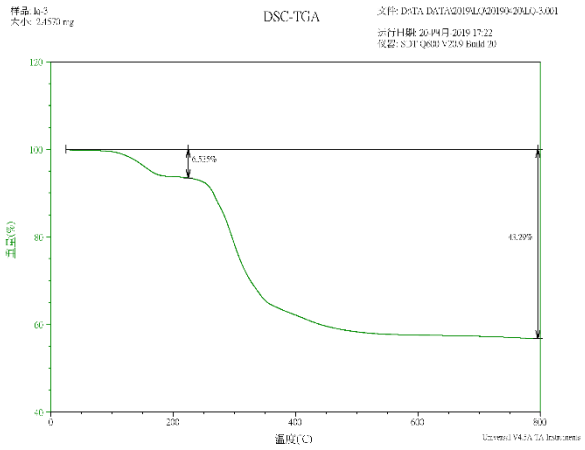

Fig. S9 The TGA curve of **4**.

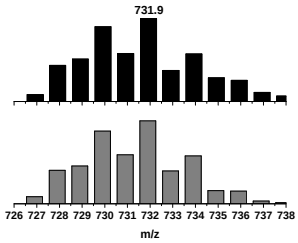

Fig. S10 The positive-ion ESI mass spectrum of $[Tp^*WS_3Cu_2(CN)_2Cu](pz)_{0.5}$ (**2**). The observed patterns (up) and the calculated isotope patterns (bottom) of the $[Tp^*WS_3Cu_2(CN)H]^+$ cation (at m/z = 731.9).

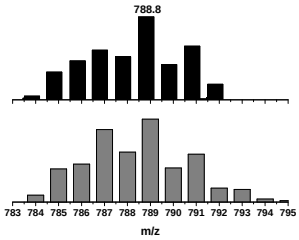

Fig. S11 The negative-ion ESI mass spectrum of $[Tp^*WS_3Cu_2(CN)_2Cu](pz)_{0.5}$ (**2**). The observed patterns (up) and the calculated isotope patterns (bottom) of the $[Tp^*WS_3Cu_2(CN)_2CH_3OH]^-$ anion (at m/z = 788.8).

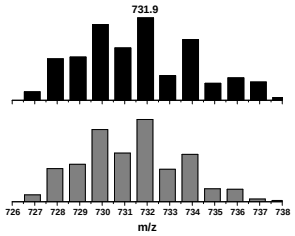

Fig. S12 The positive-ion ESI mass spectrum of $[Tp^*WS_3Cu_2(CN)_2Cu](bipy)_{0.5}$ (**3**). The observed patterns (up) and the calculated isotope patterns (bottom) of the $[Tp^*WS_3Cu_2(CN)H]^+$ cation (at m/z = 731.9).

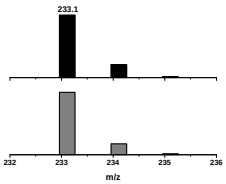

Fig. S13 The positive-ion ESI mass spectrum of $[Tp^*WS_3Cu_2(CN)_2Cu](bpb)_{0.5}$ (**4**). The observed patterns (up) and the calculated isotope patterns (bottom) of the $[bpbH]^+$ cation (at m/z = 233.1).

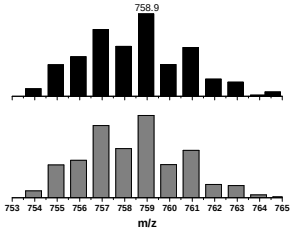

Fig. S14 The positive-ion ESI mass spectrum of $[Tp^*WS_3Cu_2(CN)_2Cu](bpb)_{0.5}$ (**4**). The observed patterns (up) and the calculated isotope patterns (bottom) of the $[Tp^*WS_3Cu_2(CN)_2H_2]^+$ cation (at m/z = 758.9).

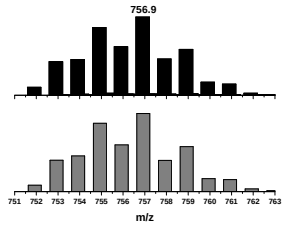

Fig. S15 The negative-ion ESI mass spectrum of $[Tp^*WS_3Cu_2(CN)_2Cu](bpb)_{0.5}$ (**4**). The observed patterns (up) and the calculated isotope patterns (bottom) of the $[Tp^*WS_3Cu_2(CN)_2]^-$ anion (at m/z = 756.9).

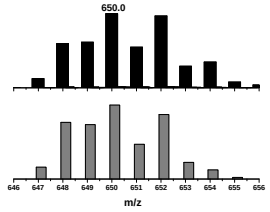

Fig. S16 The negative-ion ESI mass spectrum of $[Tp^*WS_3Cu_2(CN)_2Cu](bpb)_{0.5}$ (**4**). The observed patterns (up) and the calculated isotope patterns (bottom) of the $[Tp^*WS_3(DMF)]^-$ anion (at m/z = 650.0).

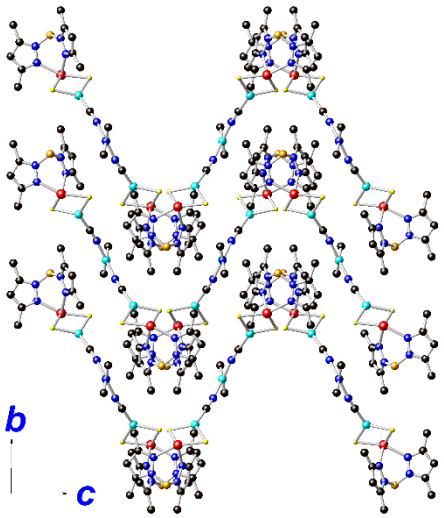

Fig. S17 Crystal packing diagram of **2** looking along the *a* direction. All hydrogen atoms are omitted. Color codes: W (red), Cu (cyan), S (yellow), N (blue), C (black), B (dark orange).

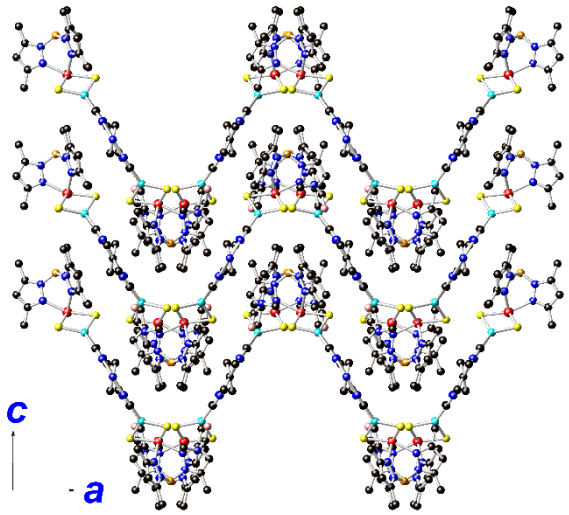

Fig. S18 Crystal packing diagram of **3** looking along the *b* direction. All hydrogen atoms are omitted. Color codes: W (red), Cu (cyan), S (yellow), N (blue), C (black), B (dark orange), O (pink).

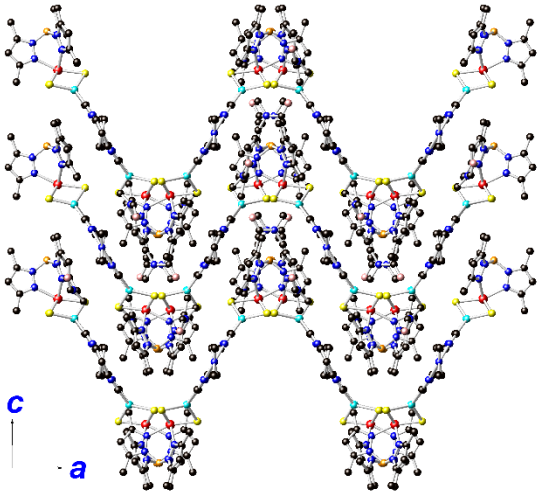

Fig. S19 Crystal packing diagram of **4** looking along the *b* direction. All hydrogen atoms are omitted. Color codes: W (red), Cu (cyan), S (yellow), N (blue), C (black), B (dark orange), O (pink).

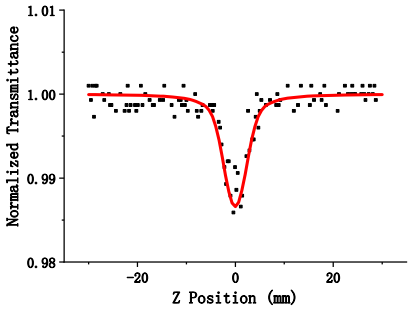

(a)

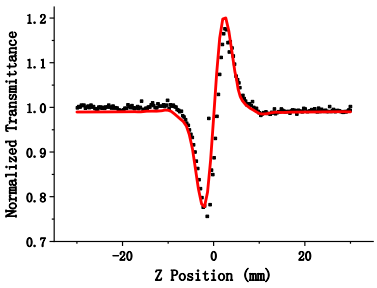

(b)

Fig. S20 *Z*-scan data of a 8.3 × 10^{-5} mol·L^{-1} solution of **3** in DMF at 532 nm. (a) Normalized *Z*-scan data under open-aperture conditions. (b) Curves obtained by dividing the normalized *Z*-scan data under closed aperture configuration by that in (a). The black squares are the experimental data, and the red solid curve is the theoretical fit.

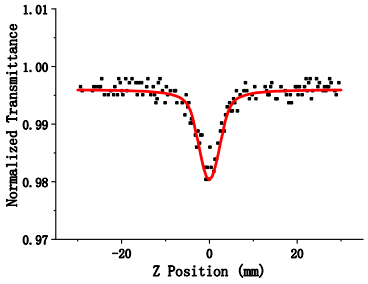

(a)

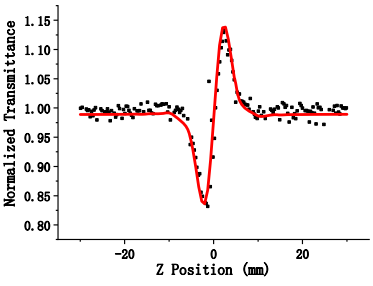

(b)

Fig. S21 *Z*-scan data of a 8.3 × 10^{-5} mol·L^{-1} solution of **4** in DMF at 532 nm. (a) Normalized *Z*-scan data under open-aperture conditions. (b) Curves obtained by dividing the normalized *Z*-scan data under closed aperture configuration by that in (a). The black squares are the experimental data, and the red solid curve is the theoretical fit.

Table S1 Selected bond lengths (Å) and angles (°) for **2**–**4**[a]

Complex **2**

W(1)-N(6)	2.239(9)	W(1)-S(2)	2.241(2)
W(1)-S(2)#1	2.241(2)	W(1)-N(4)#1	2.314(7)
W(1)-N(4)	2.314(7)	W(1)-S(1)	2.335(3)
W(1)-Cu(1)#1	2.6294(11)	W(1)-Cu(1)	2.6294(11)
Cu(1)-C(1)	1.879(9)	Cu(1)-S(2)	2.204(2)
Cu(1)-S(1)	2.216(2)	Cu(1)-Cu(1)#1	2.896(2)
Cu(2)-N(1)#2	1.896(8)	Cu(2)-N(1)	1.896(8)
Cu(2)-N(2)	2.025(11)	S(1)-Cu(1)#1	2.216(2)

N(6)-W(1)-S(2)	87.52(17)	N(6)-W(1)-S(2)#1	87.52(17)
S(2)-W(1)-S(2)#1	100.63(12)	N(6)-W(1)-N(4)#1	79.3(3)
S(2)-W(1)-N(4)#1	164.15(19)	S(2)#1-W(1)-N(4)#1	87.68(19)
N(6)-W(1)-N(4)	79.3(3)	S(2)-W(1)-N(4)	87.68(19)
S(2)#1-W(1)-N(4)	164.15(19)	N(4)#1-W(1)-N(4)	81.3(4)
N(6)-W(1)-S(1)	159.9(3)	S(2)-W(1)-S(1)	105.03(7)
S(2)#1-W(1)-S(1)	105.03(7)	N(4)#1-W(1)-S(1)	85.51(18)
N(4)-W(1)-S(1)	85.51(18)	N(6)-W(1)-Cu(1)#1	140.07(13)
S(2)-W(1)-Cu(1)#1	104.29(6)	S(2)#1-W(1)-Cu(1)#1	53.09(6)
N(4)#1-W(1)-Cu(1)#1	91.50(18)	N(4)-W(1)-Cu(1)#1	138.02(17)
S(1)-W(1)-Cu(1)#1	52.61(6)	N(6)-W(1)-Cu(1)	140.07(13)
S(2)-W(1)-Cu(1)	53.09(6)	S(2)#1-W(1)-Cu(1)	104.29(6)
N(4)#1-W(1)-Cu(1)	138.02(17)	N(4)-W(1)-Cu(1)	91.50(18)
S(1)-W(1)-Cu(1)	52.61(6)	Cu(1)#1-W(1)-Cu(1)	66.82(5)
C(1)-Cu(1)-S(2)	124.3(3)	C(1)-Cu(1)-S(1)	125.1(3)
S(2)-Cu(1)-S(1)	110.48(10)	C(1)-Cu(1)-W(1)	174.8(3)
S(2)-Cu(1)-W(1)	54.37(6)	S(1)-Cu(1)-W(1)	56.85(7)
C(1)-Cu(1)-Cu(1)#1	120.2(3)	S(2)-Cu(1)-Cu(1)#1	97.20(6)
S(1)-Cu(1)-Cu(1)#1	49.20(5)	W(1)-Cu(1)-Cu(1)#1	56.59(2)

N(1)#2-Cu(2)-N(1)	133.1(5)	N(1)#2-Cu(2)-N(2)	113.5(2)
N(1)-Cu(2)-N(2)	113.5(2)	Cu(1)-S(1)-Cu(1)#1	81.60(11)
Cu(1)-S(1)-W(1)	70.54(8)	Cu(1)#1-S(1)-W(1)	70.54(8)
Cu(1)-S(2)-W(1)	72.54(7)	C(1)-N(1)-Cu(2)	172.4(7)
C(2)#2-N(2)-Cu(2)	121.9(5)	C(2)-N(2)-Cu(2)	121.9(5)
C(6)-N(4)-W(1)	134.1(6)	N(3)-N(4)-W(1)	120.6(5)
C(11)-N(6)-W(1)	130.5(9)	N(5)-N(6)-W(1)	122.1(7)
N(1)-C(1)-Cu(1)	176.7(8)		

Complex **3**

W(1)-N(8)	2.229(4)	W(1)-S(1)	2.2333(12)
W(1)-S(3)	2.2489(12)	W(1)-N(6)	2.288(4)
W(1)-N(10)	2.317(4)	W(1)-S(2)	2.3334(11)
W(1)-Cu(2)	2.6224(6)	W(1)-Cu(1)	2.6254(6)
Cu(1)-C(1)	1.880(4)	Cu(1)-S(1)	2.1993(12)
Cu(1)-S(2)	2.2132(12)	Cu(1)-Cu(2)	2.8779(9)
Cu(2)-C(2)	1.879(5)	Cu(2)-S(3)	2.1968(13)
Cu(2)-S(2)	2.2169(12)	Cu(3)-N(1)	1.910(4)
Cu(3)-N(1)#1	1.910(4)	Cu(3)-N(3)	2.015(5)
Cu(4)-N(2)	1.889(4)	Cu(4)-N(2)#1	1.889(4)
Cu(4)-N(4)#2	2.026(6)	N(4)-Cu(4)#3	2.026(6)

N(8)-W(1)-S(1)	86.87(10)	N(8)-W(1)-S(3)	86.33(10)
S(1)-W(1)-S(3)	100.90(4)	N(8)-W(1)-N(6)	79.57(13)
S(1)-W(1)-N(6)	88.50(10)	S(3)-W(1)-N(6)	162.63(10)
N(8)-W(1)-N(10)	80.10(13)	S(1)-W(1)-N(10)	164.35(9)
S(3)-W(1)-N(10)	86.98(9)	N(6)-W(1)-N(10)	80.68(13)
N(8)-W(1)-S(2)	161.42(10)	S(1)-W(1)-S(2)	105.05(4)
S(3)-W(1)-S(2)	104.86(4)	N(6)-W(1)-S(2)	86.45(9)
N(10)-W(1)-S(2)	85.65(9)	N(8)-W(1)-Cu(2)	138.99(10)
S(1)-W(1)-Cu(2)	103.72(3)	S(3)-W(1)-Cu(2)	52.94(3)

N(6)-W(1)-Cu(2)	139.08(9)	N(10)-W(1)-Cu(2)	91.84(9)
S(2)-W(1)-Cu(2)	52.76(3)	N(8)-W(1)-Cu(1)	139.60(10)
S(1)-W(1)-Cu(1)	53.08(3)	S(3)-W(1)-Cu(1)	104.53(3)
N(6)-W(1)-Cu(1)	92.80(9)	N(10)-W(1)-Cu(1)	138.18(9)
S(2)-W(1)-Cu(1)	52.62(3)	Cu(2)-W(1)-Cu(1)	66.516(19)
C(1)-Cu(1)-S(1)	124.43(13)	C(1)-Cu(1)-S(2)	124.98(13)
S(1)-Cu(1)-S(2)	110.46(5)	C(1)-Cu(1)-W(1)	175.26(13)
S(1)-Cu(1)-W(1)	54.28(3)	S(2)-Cu(1)-W(1)	56.90(3)
C(1)-Cu(1)-Cu(2)	120.49(13)	S(1)-Cu(1)-Cu(2)	96.91(4)
S(2)-Cu(1)-Cu(2)	49.54(3)	W(1)-Cu(1)-Cu(2)	56.691(16)
C(2)-Cu(2)-S(3)	123.17(16)	C(2)-Cu(2)-S(2)	125.73(16)
S(3)-Cu(2)-S(2)	110.77(5)	C(2)-Cu(2)-W(1)	175.80(16)
S(3)-Cu(2)-W(1)	54.78(3)	S(2)-Cu(2)-W(1)	56.92(3)
C(2)-Cu(2)-Cu(1)	121.70(14)	S(3)-Cu(2)-Cu(1)	98.21(4)
S(2)-Cu(2)-Cu(1)	49.43(3)	W(1)-Cu(2)-Cu(1)	56.793(16)
N(1)-Cu(3)-N(1)#1	130.8(2)	N(1)-Cu(3)-N(3)	114.58(12)
N(1)#1-Cu(3)-N(3)	114.58(12)	N(2)-Cu(4)-N(2)#1	133.1(3)
N(2)-Cu(4)-N(4)#2	113.43(14)	N(2)#1-Cu(4)-N(4)#2	113.43(14)
Cu(1)-S(1)-W(1)	72.64(4)	Cu(1)-S(2)-Cu(2)	81.03(4)
Cu(1)-S(2)-W(1)	70.49(3)	Cu(2)-S(2)-W(1)	70.33(3)
Cu(2)-S(3)-W(1)	72.28(4)	C(1)-N(1)-Cu(3)	174.1(4)
C(2)-N(2)-Cu(4)	174.6(4)	C(3)#1-N(3)-Cu(3)	121.3(3)
C(3)-N(3)-Cu(3)	121.3(3)	C(8)#1-N(4)-Cu(4)#3	121.5(3)
C(8)-N(4)-Cu(4)#3	121.5(3)	C(12)-N(6)-W(1)	132.9(3)
N(5)-N(6)-W(1)	121.5(3)	C(17)-N(8)-W(1)	131.7(3)
N(7)-N(8)-W(1)	121.8(3)	C(22)-N(10)-W(1)	133.2(3)
N(9)-N(10)-W(1)	120.9(3)	N(1)-C(1)-Cu(1)	175.7(4)
N(2)-C(2)-Cu(2)	176.6(4)		

Complex **4**

W(1)-N(8)	2.224(9)	W(1)-S(1)	2.234(3)
W(1)-S(3)	2.250(3)	W(1)-N(6)	2.279(10)
W(1)-N(10)	2.311(10)	W(1)-S(2)	2.333(3)
W(1)-Cu(2)	2.6190(16)	W(1)-Cu(1)	2.6260(16)
Cu(1)-C(1)	1.887(12)	Cu(1)-S(1)	2.196(3)
Cu(1)-S(2)	2.218(3)	Cu(1)-Cu(2)	2.890(2)
Cu(2)-C(2)	1.865(14)	Cu(2)-S(3)	2.197(4)
Cu(2)-S(2)	2.217(3)	Cu(3)-N(1)#1	1.911(12)
Cu(3)-N(1)	1.911(12)	Cu(3)-N(3)	1.996(17)
Cu(4)-N(2)	1.919(11)	Cu(4)-N(2)#1	1.919(11)
Cu(4)-N(4)#2	1.995(17)	N(4)-Cu(4)#3	1.995(17)

N(8)-W(1)-S(1)	86.6(3)	N(8)-W(1)-S(3)	86.8(3)
S(1)-W(1)-S(3)	101.00(12)	N(8)-W(1)-N(6)	78.8(4)
S(1)-W(1)-N(6)	88.7(3)	S(3)-W(1)-N(6)	162.2(3)
N(8)-W(1)-N(10)	79.9(3)	S(1)-W(1)-N(10)	164.3(3)
S(3)-W(1)-N(10)	86.5(3)	N(6)-W(1)-N(10)	80.7(4)
N(8)-W(1)-S(2)	161.1(3)	S(1)-W(1)-S(2)	105.09(11)
S(3)-W(1)-S(2)	104.95(12)	N(6)-W(1)-S(2)	86.6(3)
N(10)-W(1)-S(2)	86.0(2)	N(8)-W(1)-Cu(2)	139.5(3)
S(1)-W(1)-Cu(2)	103.87(9)	S(3)-W(1)-Cu(2)	52.98(9)
N(6)-W(1)-Cu(2)	139.2(2)	N(10)-W(1)-Cu(2)	91.7(2)
S(2)-W(1)-Cu(2)	52.79(8)	N(8)-W(1)-Cu(1)	139.2(3)
S(1)-W(1)-Cu(1)	52.98(9)	S(3)-W(1)-Cu(1)	104.86(9)
N(6)-W(1)-Cu(1)	93.0(3)	N(10)-W(1)-Cu(1)	138.7(2)
S(2)-W(1)-Cu(1)	52.73(8)	Cu(2)-W(1)-Cu(1)	66.86(5)
C(1)-Cu(1)-S(1)	124.2(4)	C(1)-Cu(1)-S(2)	125.2(4)
S(1)-Cu(1)-S(2)	110.47(13)	C(1)-Cu(1)-W(1)	175.8(4)
S(1)-Cu(1)-W(1)	54.31(9)	S(2)-Cu(1)-W(1)	56.84(8)
C(1)-Cu(1)-Cu(2)	121.4(4)	S(1)-Cu(1)-Cu(2)	96.70(11)

S(2)-Cu(1)-Cu(2)	49.31(9)	W(1)-Cu(1)-Cu(2)	56.45(5)
C(2)-Cu(2)-S(3)	124.2(5)	C(2)-Cu(2)-S(2)	124.5(5)
S(3)-Cu(2)-S(2)	110.91(13)	C(2)-Cu(2)-W(1)	177.1(5)
S(3)-Cu(2)-W(1)	54.87(9)	S(2)-Cu(2)-W(1)	56.97(8)
C(2)-Cu(2)-Cu(1)	121.9(4)	S(3)-Cu(2)-Cu(1)	98.21(11)
S(2)-Cu(2)-Cu(1)	49.36(9)	W(1)-Cu(2)-Cu(1)	56.69(5)
N(1)#1-Cu(3)-N(1)	129.7(7)	N(1)#1-Cu(3)-N(3)	115.2(3)
N(1)-Cu(3)-N(3)	115.2(3)	N(2)-Cu(4)-N(2)#1	135.2(7)
N(2)-Cu(4)-N(4)#2	112.4(4)	N(2)#1-Cu(4)-N(4)#2	112.4(4)
Cu(1)-S(1)-W(1)	72.71(10)	Cu(2)-S(2)-Cu(1)	81.33(11)
Cu(2)-S(2)-W(1)	70.23(9)	Cu(1)-S(2)-W(1)	70.43(9)
Cu(2)-S(3)-W(1)	72.15(11)	C(1)-N(1)-Cu(3)	173.6(11)
C(2)-N(2)-Cu(4)	174.5(13)	C(3)#1-N(3)-Cu(3)	121.9(8)
C(3)-N(3)-Cu(3)	121.9(8)	C(12)-N(4)-Cu(4)#3	122.1(11)
C(12)#1-N(4)-Cu(4)#3	122.1(11)	C(16)-N(6)-W(1)	132.5(8)
N(5)-N(6)-W(1)	121.9(8)	N(7)-N(8)-W(1)	122.8(7)
C(21)-N(8)-W(1)	130.8(8)	N(9)-N(10)-W(1)	120.9(8)
C(26)-N(10)-W(1)	133.2(8)	N(1)-C(1)-Cu(1)	175.0(11)
N(2)-C(2)-Cu(2)	174.4(13)		

[a] Symmetry codes for **2**: #1 –*x*, *y*, *z*; #2 *x*, –*y* + 1, –*z*; #3 –*x* + 1, *y*, *z*; for **3**: #1 –*x*, *y*, –*z*– 1/2; #2 *x*, *y* + 1, *z*; #3 *x*, *y* – 1, *z*; for **4**: #1 –*x* + 2, *y*, –*z* + 1/2; #2 *x*, *y* + 1, *z*; #3 *x*, *y* – 1, *z*.